IEEE Access
Multidisciplinary | Rapid Review | Open Access Journal

Received May 26, 2019, accepted September 9, 2019, date of publication October 28, 2019, date of current version November 6, 2019.

Digital Object Identifier 10.1109/ACCESS.2019.2944737

Performance Prediction of Hatch Cover Drive Assembly in Space Environment

PAN BO[1] (Member, IEEE), CHI CHENG[2], HE YONGQIANG[1], ZHANG SHUYANG[1], ZHANG PUZHEN[1], ZHANG DONGHUA[1], AND CHI GUANXIN[2], (Member, IEEE)

[1]Beijing Institute of Spacecraft System Engineering, Beijing 100094, China
[2]Harbin Institute of Technology, Harbin 150001, China

Corresponding author: Chi Guanxin (chigx@hit.edu.cn)

This work was supported by the National Natural Science Foundation of China under Project 51605028.

ABSTRACT The performance of the Hatch Cover Drive Assembly operated in space is quite important for aircrafts. However, it is hard to experimental studies in space. As an alternative, theoretical analysis and simulation are employed to predict their performances on the ground. Herein, a mathematical model of the drive assembly was first established and simulated in Matlab. The armature current and mechanical efficiency were analyzed with respect to the operating temperature and load torque. Furthermore, a test setup according to the model was built to verify the validity of the proposed mathematical model. As a result, the prediction results are consistent with the experimental results very well with a maximum error of 11.0% in the armature current and 11.6% in the mechanical efficiency. The mechanical efficiency achieves to be the maximum value in vacuum as the load torque of 3.5N·m. It has the best performance as working around the room temperature. The proposed model would be used to predict the performance of drive assembly working in space. Our findings would be helpful for the designing, manufacturing and selection of motors and reducers for spacecrafts usage in future.

INDEX TERMS Drive Assembly, performance prediction, brushless dc motor, harmonic reducer, space environment.

I. INTRODUCTION

Motors and reducers are the key components of the drive assembly of spacecrafts, which drive the payloads and functional components for finishing the specified actions and motions in space [1], [2]. Up to now, many kinds of motors and reducers are developed to fulfill the various missions, among them, the brushless DC motor driven by DC converter is widely used in aerospace due to its simple structure, reliable operation and long service life [3], [4]. In addition, the DC motor can drive a large load combined with the harmonic reducer. This drive assembly shows many advantages of the large transmission ratio, small mass and volume, high transmission accuracy, and is quite suitable for application in spatial motion [5], [7].

However, the special environment in space would degenerate the performance of the drive assembly of DC motor and harmonic reducer, resulting in a lot of disasters. For instance, the coil resistance and magnetic destiny in the motor, and the grease viscosity in harmonic reducer, are changed heavily upon the alternating of high and low temperature. As a result, the coupling effect of these factors highly degenerates the output performance of the drive assembly.

Many studies have focused on these problems, but limited to DC motor or reducer or environment simulation technology [8], [9] rather than the drive assembly. Some scholars have carried out in-depth research on parameters, rotational speed, calculation of back EMF coefficient, thermal analysis and circuit control of brushless DC motor [10], [22]. Among them, SUN carried out high and low temperature tests on PMSM from an engineering perspective, and verified the approximate linear relationship between back EMF coefficient and temperature [19]. ZHANG established the formula for calculating the back EMF coefficient in the design of brushless DC torque motor [20]. Capponi et al revised the motor model, predicted and verified the back EMF and control current [21]. SUN proposed a design method of motor in high temperature environment [22]. Some scholars have also studied the influence of the influence of space harmonic transmission lubrication and vacuum grease on the performance of harmonic reducer [23], [28], in particular, K. Zhao studied the testing method of harmonic performance in high

The associate editor coordinating the review of this manuscript and approving it for publication was Rosario Pecora.

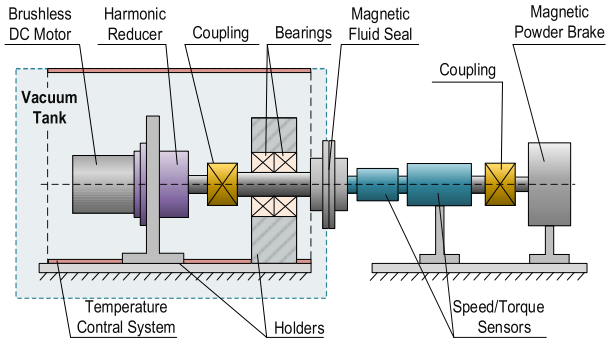

FIGURE 1. Diagram of experimental system model.

and low temperature environment and conducted experiments [26]. LI et al carried out 601EF grease experimental study on the performance of harmonic gear transmission in vacuum thermal cycle environment [27]. K. Maniwa and S. Obara found that poor lubrication effect in vacuum environment is an important factor leading to the reduction of transmission efficiency of harmonic reducer [28].

Herein, the Hatch Cover driving assembly consisting of the brushless DC motor and harmonic reducer (XBS-32-80) is first set up. The corresponding mathematical model of the armature current and mechanical efficient is descried. Both parameters show a nonlinear relationship with respect to environment temperature. Furthermore, the experimental results show a good agreement to the values calculated from the mathematical models, suggesting a quite good prediction ability of our models. The influence of motor temperature rise on driving assembly is neglected in this study due to the short duration of operation.

II. RESEARCH METHOD

Figure 1 illustrates the scheme of our setup, from which the mathematical models of the drive assembly is established. In brief, the drive assembly contains the brushless DC motor, harmonic reducer, necessary supports and connection assembly (**Figure 1**), which are arranged in the thermal vacuum tank. The loaded magnetic powder brakes, torque and speed sensors, drivers and controllers are arranged outside the thermal vacuum tank (Figure 1). The magnetic fluid seal is used for the output shaft sealing. It worthy noted that the influence of the vacuum on the performance of the drive assembly is neglected. Only the temperature is our object. As a result, the procedure is depicted in **Figure 2**.

Generally, the drive assembly model contains two parts: the motor model and load model. The former mainly contains the terminal voltage, coil resistance, coil inductance, magnet remanence and back-EMF of brushless DC motor. The effect of temperature on the coil resistance, coil inductance, magnet remanence and back-EMF were especially identified. In the later, the transmission efficiency of the reducer and rotary resistance torque of other components were considered. The effect of temperature on the grease viscosity and rotary resistance torque were also introduced. The mechanical efficiency and power consumption would be predicated by building

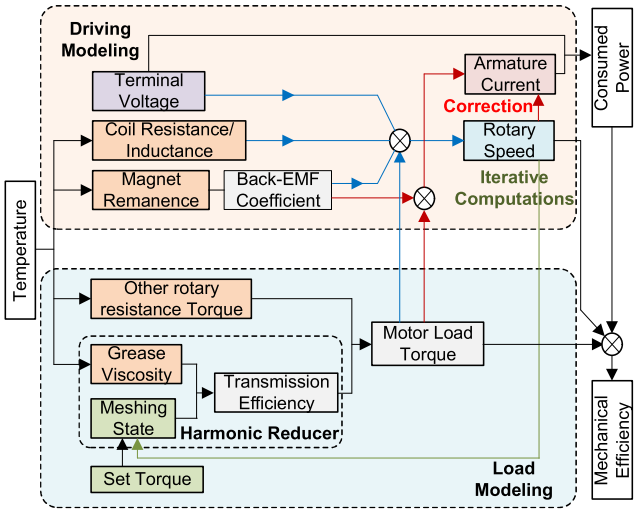

FIGURE 2. Diagram of the influence of temperature on drive assembly.

TABLE 1. Technical index of brushless DC motor.

Projects	Technical index
Service voltage/V	+28
Number of pole pairs	3
Rated speed/rpm	2500
Rated torque/ $\mathrm{N}\cdot\mathrm{m}$	0.07
Rated current/A	1.1
Rated power/W	28
Stator coil resistance/Ω	6

TABLE 2. Technical index of harmonic reducer.

Projects	Technical index
Transmission ratio	80
Modulus	0.2
Rated input speed/rpm	2500
Rated output torque/ $\mathrm{N}\cdot\mathrm{m}$	5
Maximum output torque/ $\mathrm{N}\cdot\mathrm{m}$	7
Input speed range/rpm	0～3000

armature current model, rotary speed model and motor load torque. Herein the armature current model is equal to power consumption model considering that the terminal voltage is a constant. Therefore, we will only discuss the armature current model and the mechanical efficiency.

III. MODELING AND SIMULATION

A. MODEL OF DRIVE ASSEMBLY

The mathematical model of drive assembly is carried out by modeling the brushless motor and drive load separately to describe the effect of temperature on the armature current.

Table 1 and **2** lists the basic data of the brushless DC motor and harmonic reducer.

All the supporting bearings are the deep groove ball bearing, and lubricated by solid state. Permanent magnet material in the brushless DC motor is 2-17SmCo with good temperature stability [18]. The harmonic reducer is lubricated with 601EF vacuum grease with good viscosity and temperature performance [27].

1) MODEL ESTABLISHMENT OF BRUSHLESS DC MOTOR

Assuming that the magnetic circuit of the brushless DC motor is unsaturated, the resistance of different windings is equal, and the power semiconductor devices in the inverters are the same. The voltage equation of star-connected brushless DC motor can be derived as follows:

$$\begin{bmatrix} u_a \\ u_b \\ u_c \end{bmatrix} = \begin{bmatrix} r & 0 & 0 \\ 0 & r & 0 \\ 0 & 0 & r \end{bmatrix} \begin{bmatrix} i_a \\ i_b \\ i_c \end{bmatrix} + \begin{bmatrix} L & M & M \\ M & L & M \\ M & M & L \end{bmatrix} \times \frac{d}{dt} \begin{bmatrix} i_a \\ i_b \\ i_c \end{bmatrix} + \begin{bmatrix} e_a \\ e_b \\ e_c \end{bmatrix} \tag{1}$$

where, u_a, u_b, u_c are the three phases voltage i_a, i_b, i_c are the three phases currents, e_a, e_b, e_c are the three phases back electromotive forces (back-EMF), respectively. L, M are the self-inductance and mutual-inductance, r is the single winding resistance value.

According to the conservation of energy, the electromagnetic torque equation is obtained as follows:

$$T_e = \frac{e_a i_a + e_b i_b + e_c i_c}{\omega} \tag{2}$$

The amplitude of the motor's back-EMF is determined by the motor rotating speed of n and the back-EMF coefficient of K_e. Generally, K_e is considered as a constant while the motor structure is determined. However, the variation of temperature in space will influence the air gap magnetic density, leading to the change of coefficient K_e.

$$E = K_e(T) \cdot n \tag{3}$$

In consideration of the influence of the winding inductance on the armature current, a correction factor K_a is introduced as [10], [11]:

$$K_a = 1 - \frac{Pn\tau}{10}\left(\frac{e^{\frac{10}{Pn\tau}} - 1}{2e^{\frac{10}{Pn\tau}} - 1}\right) \tag{4}$$

where, P is the number of pole pairs in the motor, τ is the electromagnetic time constant.

According to the Eq.(2-4), the function of armature current can be obtained.

$$I = \frac{\pi K_a}{30K_e(T)} \cdot T_e \tag{5}$$

According to the Eq.(1) and Eq.(3), the expression of motor rotate speed $n(T)$ can be obtained:

$$n = \frac{U - I \cdot r(T)}{K_e(T)} \tag{6}$$

where, U is the effective value of the terminal voltage.

Previous results [13], [17] revealed an approximate linear relationship between the back EMF coefficient K_e and the work temperature T within the operating temperature range of the drive assembly. Therefore, we defined $K_e(T)$ as follow:

$$K_e(T) = \lambda_t T + b \tag{7}$$

where, λ_t and b are 0.006667 and 8.16667 given by manufacturer respectively.

Finally, the armature current I and rotate speed n can be solved by substituting Eq.(7) to Eq.(5) and (6). The relationship between the I, n and the environment temperature T and the electromagnetic torque T_e. are set up.

2) MODEL OF DRIVE LOAD

According to the experimental system model, the load is driven by the electromagnetic torque (T_e) of the brushless DC motor. It contains the resistance torque given by two support bearings inside the motor (T_{n1}) and (T_{n2}), two supporting shaft bearings (T_c), the magnetic fluid seal (T_m), and constant torque for magnetic powder braking(T_0). Combining the deceleration ratio of harmonic reducer (i) with the transmission efficiency (η_T), the torque balance equation in steady-state rotation is derived:

$$(T_e - T_{n1} - T_{n2}) \cdot i \cdot \eta_T = 2T_c + T_m + T_0 \tag{8}$$

Then, T_e can be obtained:

$$T_e = \frac{2T_c + T_m + T_0}{i \cdot \eta_T} + T_{n1} + T_{n2} \tag{9}$$

Generally, the resistance torques T_c, T_{n1} and T_{n2} vary with the motor speed and temperature, but the change can be reasonably neglected. Meanwhile the change of the magnetic fluid seal (T_m) has also been confirmed to be a small scope according to the measurement results at different temperatures.

It is well known that the transmission efficiency (η_T) is affected by temperature (T), rotation speed (n) and load torque (T_r) [23]:

$$\eta_T = (T, n(T), T_r) \tag{10}$$

where, the load torque T_r is:

$$T_r = 2T_c + T_m + T_0 \tag{11}$$

According to original experimental data at 20 °C collected from the manufacturer, the fitting model of transmission efficiency F_{nt} (n, T_r, $T = T_{con}$) is obtained. **Figure 3** depicts the relationship of load torque, input speed and transmission

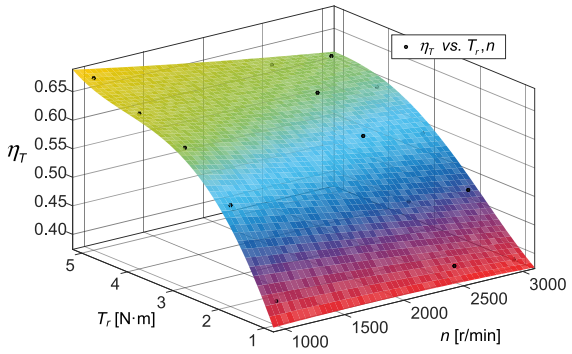

FIGURE 3. Effect of rotation speed and load torque on transmission efficiency at room temperature.

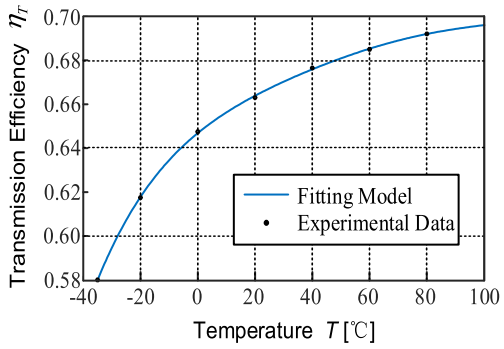

FIGURE 4. The relation between transmission efficiency of harmonic reducer and temperature.

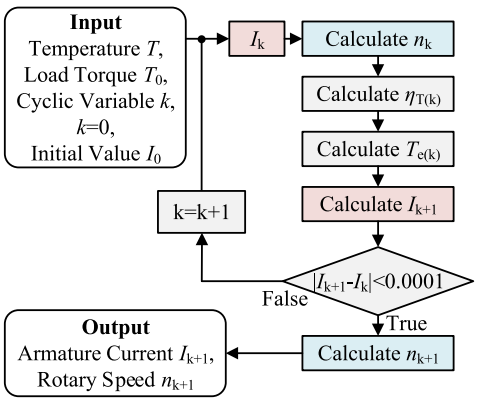

FIGURE 5. Flow chart of model solving process.

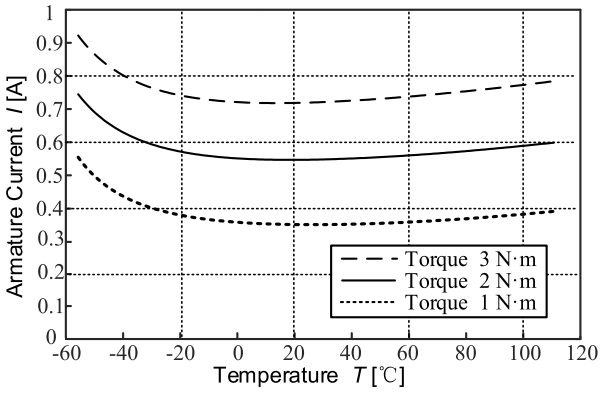

FIGURE 6. Theoretical model of armature current-temperature relationship under different loads.

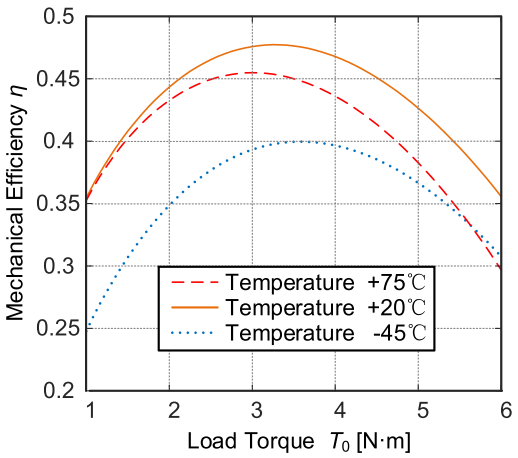

FIGURE 7. Theoretical model of load torque-mechanical efficiency.

efficiency at room temperature. **Figure 4** plots the transmission efficiency fitting model $F_T(T)$ of harmonic reducer as a function of operating temperature while the load torque and rotation speed are constants.

To simplify the transmission efficiency model of each harmonic reducer, we assume that the temperature has the same effect on the efficiency at the arbitrary speed and torque. As a result, the model of transmission efficiency(η_T) was proposed as follows:

$$\eta_T = F_{nt}(n, T_r) \cdot \left(1 + \frac{F(T) - F(T_{con})}{F(T_{con})}\right) \tag{12}$$

B. PREDICT AND ANALYSIS OF DRVIE ASSEMBLY

Based on the Eq. (6) and (12), the predict models of armature current and mechanical efficiency of drive assembly are written as follow:

$$I = \frac{\pi K_a}{30K_e}\left(\frac{2T_c + T_m + T_0}{i \cdot \eta_T} + T_{n1} + T_{n2}\right) \tag{13}$$

$$\eta = \frac{n\pi T_r}{30UI} \times 100\% \tag{14}$$

Usually, the armature current (I) and electromagnetic torque (T_e) are coupled, the solution has to be solved iteratively. **Figure 5** shows the diagram of the solving process, which is realized in Matlab software.

Figure 6 plots the I with respect to T as the setting torque of 1, 2 and 3 N·m respectively. All the curves show a concave shape with the lowest point at around 20°C. The increasing I both at higher and lower temperature can be explained by two reasons. In the low temperature range, the increasing grease viscosity in the reducer is response to the sharply increasing of I. It has more power loss, which coincides with the efficiency curve of the reducer. While in the high temperature range, the magnetism weakening in the motor may increase the I, which means high current is required for the end-effector.

Figure 7 plots the mechanical efficiency with respect to the load torque at the temperature of 75°C, 20°C and −45°C, respectively.

For all the testing temperatures, the efficiency increases first and then decreases with the increase of load torque. The output torque decreases at the maximum efficiency of the drive assembly, when the temperature increases, and increases at the maximum efficiency of the drive assembly when the temperature decreases. The effect of the operating temperature on the efficiency of drive assembly is much higher in the low temperature range compared with that in the high temperature range. That means the reducer has greater influence on the performance of the drive assembly. Although the output torque of the drive assembly at the maximum efficiency at low temperature is larger than

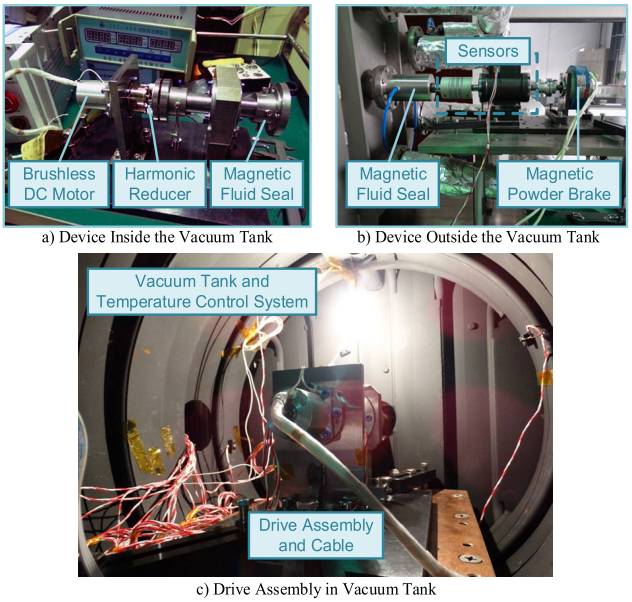

a) Device Inside the Vacuum Tank
b) Device Outside the Vacuum Tank
c) Drive Assembly in Vacuum Tank

FIGURE 8. Test system.

TABLE 3. Details of experimental conditions.

Projects		Conditions
Vacuum degree/P_a		$\leq 6.65\times10^{-3}$
Temperature/℃		-55、-45、20、75*1
Load torque/(N·m)		1～6
Residence time per measurement /*min*		2
Motor input voltage	Voltage /V	28
	Duty cycle/%	90%
Temperature deviation allowed	High temperature/℃	0～4
	Low temperature/℃	-4～0
Duration deviation allowed		0～10%

*1 Set by project practice experiment and predict model, -55℃ is added for a low temperature.

that at high temperature, the overall mechanical efficiency is lower. Therefore, it should be avoided to work at lower temperature.

IV. EXPERIMENTS

To reveal the temperature influence on the motor current and the mechanical efficiency of the drive assembly, a test system is built according to the model in **Figure 1**. **Figure 8** shows a digital picture of setup, which includes the brushless DC motor, harmonic reducer, coupling, adapter shaft, supporting bearing, vacuum tank, magnetic powder brake, magnetic fluid seal, adapter shaft, temperature sensor, torque sensor and speed sensor. To simulate the space environment, the drive assembly was placed in a vacuum tank, where the temperature was controlled by the electric heating and liquid nitrogen flowing.

To achieve the normal working performance, the drive assembly was run in advance to ensure that the grease evenly diffuses into the contact parts of the rigid wheel and the flexible wheel tooth surface. The experimental data is accumulated in **Table 3**.

TABLE 4. Results of experiment and prediction on armature current.

Torque (N·m)	Temp. (℃)	Exp. (A)	Pre. (A)	Error (%)
1	-55	0.5050	0.5548	9.86%
	-45	0.4475	0.4691	4.83%
	+20	0.4000	0.3561	11.0%
	+75	0.4125	0.3708	10.1%
2	-55	0.7125	0.7412	4.03%
	-45	0.6150	0.6580	6.99%
	+20	0.5500	0.5472	0.51%
	+75	0.5925	0.5698	3.83%
3	-55	0.9450	0.9143	3.25%
	-45	0.7900	0.8281	4.82%
	+20	0.7100	0.7153	0.75%
	+75	0.7725	0.7459	3.44%

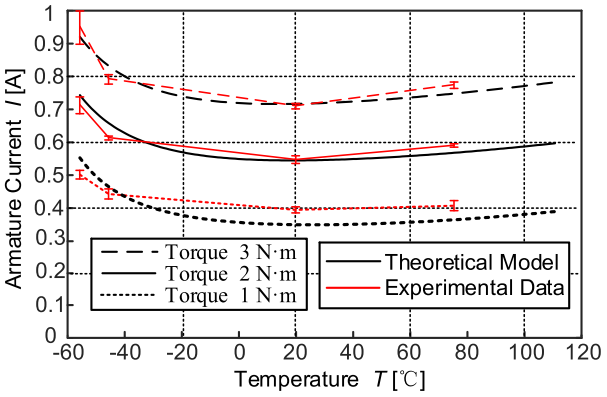

FIGURE 9. Diagram of experimental and theoretical curves of armature current varying with temperature.

During the tests, the vacuum value, input voltage of motor and duty cycle were kept unchanged, each test was performed after keeping the target temperature for 2 hours at least and the results were the average of three experimental results.

V. EXPERIMENTAL RESULTS AND ANALYSIS

The armature current I were measured with respect to the torque (1, 2, 3N.m). The results and predictions were accumulated in **Table 4** and plotted in **Figure 9**.

In the mechanical efficiency experiments, the load torque was changed from 1 to 6N·m at three operating temperatures, while the armature current of the brushless DC motor and rotate speed were recorded. The mechanical efficiency were acquired through Eq.(14). The measurement and prediction values were listed in **Table 5**. The experimental and theoretical curves of mechanical efficiency varying with load torque were plotted in **Figure 10**.

Figure 9 and 10 show that the prediction results are consistent with the experiment results very well with a maximum error of 11.0% in the armature current and 11.6% in the mechanical efficiency. The maximum prediction error of the armature current occurs at the load torque of 1N·m, while it is 5N·m for the maximum prediction error of mechanical efficiency Meanwhile, the mechanical efficiency reaches its maximum value when the load torque is around 3.5N·m. Both in the high and low temperature range, the mechanical efficiency are lower than that in the normal temperature. Fur-

TABLE 5. Results of experiment and prediction on efficiency.

Torque (N·m)	Temp. (°C)	Exp.	Pre.	Error (%)
1	+75	0.3504	0.3526	0.63%
	-45	0.2648	0.2478	6.42%
	+20	0.3532	0.3545	0.37%
2	+75	0.4051	0.4327	6.81%
	-45	0.3649	0.3486	4.47%
	+20	0.4533	0.4434	2.18%
3	+75	0.4371	0.4549	4.07%
	-45	0.3970	0.3932	0.96%
	+20	0.4916	0.4759	3.19%
4	+75	0.4045	0.4361	7.81%
	-45	0.3762	0.3966	5.42%
	+20	0.4832	0.4678	3.19%
5	+75	0.3552	0.3827	7.74%
	-45	0.3285	0.3666	11.6%
	+20	0.4639	0.4265	8.06%

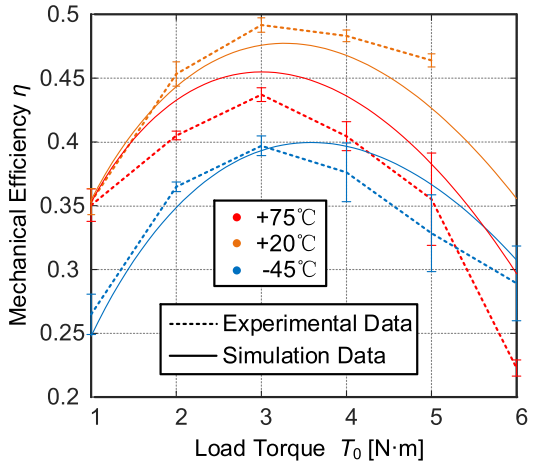

FIGURE 10. Diagram of torque-mechanical efficiency experimental.

thermore the mechanical efficiency decreased significantly at low temperature range.

The causes of prediction errors may be explained as follows:

1) The heating of motor during operating, results in a higher temperature in motor compared with that in the around environment. In addition, there is temperature gradient in the reducer. These facts make the setting parameters in the prediction model different from their actual values.

2) The transmission efficiency of the model of the harmonic reducer is a hypothesis according to the manufacture's experimental data at room temperature.

3) The resistance torques of T_c, T_{n1}, T_{n2} and the magnetic fluid seal T_m vary with the motor speed and temperature, but they were considered as constant in our model,.

VI. CONCLUSION

According to the mathematical model and experimental results, the following conclusions can be drawn:

1) The prediction results are consistent with the experiment results very well with a maximum error of 11.0% in the armature current and 11.6% in the mechanical efficiency. It would be used to predict the performance of drive assembly working in the airspace.

2) The proposed liner model of back EMF coefficient and the fitting model of transform efficiency of reducer based on manufacturer experiment data can still meet practical application, although some prediction errors exist.

3) When operating in the low temperature range, the frictional additional torque of harmonic reducer, which sharply increases with the viscosity of grease decreases rapidly, is the main factor affecting the armature current of the drive assembly. When operating in the high temperature range, the weakening of permanent magnet is the main factors affecting the armature current of the drive assembly.

4) The mechanical efficiency achieves to be the maximum in vacuum as the load torque of 3.5N·m. It has the best performance as working around the room temperature.

In summary, we proposed a mathematical model to predict the armature current and mechanical efficiency of the space drive assembly under the specified working conditions. Experimental results prove that the proposed model has a good prediction accuracy with a maximum error of 11.0% in the armature current and 11.6% in the mechanical efficiency. Our findings would be helpful for the designing, manufacturing and selection of motors and reducers for spacecrafts usage in future.

ACKNOWLEDGMENT

Thanks Beijing Satellite Manufacturing Factory for their help in the test process.

REFERENCES

[1] F. B. Oswald, "Space mechanisms technology workshop," NASA, Washington, DC, USA,, Tech. Rep. CP-210971, Jun. 2001, no. 2.
[2] H. Hu, B. Pan, and J. Sun, "Friction torque modeling of spacecraft driving mechanism shafting," *J. Mech. Eng.*, vol. 53, no. 11, pp. 75–80, Jun. 2017.
[3] J. C. Tan, *Permanent Magnet Brushless DC Motor Technology*. Beijing, China: China Machine Press, 2011.
[4] J. Luo, J. Fan, Y. Si, T. Sun, and A. Shang, "Driving performance investigation on ultrasonic motor under vacuum and high-low temperature environment," *J. Vib., Meas. Diagnosis*, vol. 38, no. 2, pp. 376–380, Apr. 2018.
[5] H. Zhou, Q. P. Wen, and W. W. Zhang, "Harmonic driver used in spacecraft," *Vac. Cryogenics*, vol. 10, no. 4, pp. 187–192, Dec. 2004.
[6] K. Ueura and R. Slatter, "ACTUATORS: Development of the harmonic drive gear for space applications," in *Proc. Eur. Space Mech. Tribol. Symp. (ESMATS)*, Sep./Oct. 1999, pp. 259–264.
[7] W. M. Liu, L. J. Weng, and J. Y. Sun, *Space Lubrication Materials and Technology Manual*. Beijing, China: Science Press, 2009.
[8] X. Wang, "Present status and development of environment simulation technology in China," *Aeronaut. Manuf. Technol.*, vol. 8, pp. 49–52, Aug. 2004.
[9] D. D. Li, "Simulation and experiment research about temperature and flow field in low/high temperature environment testing system," Ph.D. dissertation, Dept. Power Eng. Eng. Therm. Phys., Shanghai Jiao Tong Univ., Shanghai, China, 2015.
[10] N. N. Tian, "Finite element modeling and multi-field coupling analysis of BLDC wheel motor," Ph.D. dissertation, Dept. Vehicle Eng., Jilin Univ., Changchun, China, 2014.
[11] J.-C. Tan, "Commutation process analysis of brushless DC motor and analytical expression of average current and average electromagnetic torque," *Micromotors*, vol. 43, no. 5, pp. 13–18, May 2010.
[12] K.-P. Li, Q. S. Hu, and Y. K. Huang, "The circuit model of the permanent-magnet brushless DC motor allowing for its windings inductances and its analysis," *Proc. CSEE*, vol. 24, no. 1, pp. 76–80, Jan. 2004.

[13] X. Z. Zhang and J. W. Guo, "Measurement and analysis of the inductances of PM brushless DC motor," *Micromotors*, vol. 44, no. 5, pp. 88–92, May 2011.
[14] X. H. Wei, C. H. Wen, and T. H. Tang, "Analysis of The influence of brushless DC motor parameters on its rotation speed," *Shanghai Medium Lager Electr. Mach.*, no. 3, pp. 16–19, Mar. 2008.
[15] N. Takahashi, M. Morishita, D. Miyagi, and M. Nakano, "Examination of magnetic properties of magnetic materials at high temperature using a ring specimen," *IEEE Trans. Magn.*, vol. 46, no. 2, pp. 548–551, Feb. 2010.
[16] G. Du, H. Wang, Y. Wang, and X. Liu, "Multiphysics thermal analysis of a high speed permanent magnet brushless DC motor," in *Proc. Int. Conf. Elect. Mach. Syst.*, Aug. 2011, pp. 1–5.
[17] J. H. Hu, J. B. Zou and S. L. Jiang, "Design of a high temperature brushless DC motor drive and control circuit for oil well detecting," *Chin. J. Electron Devices*, vol. 29, no. 2, pp. 528–531, Jun. 2006.
[18] L. L. Zou, B. Y. Huang, and J. H. Yi, "Influence of temperature on The magnetic properties of 2:17 type SmCo permanent magnets," *Powder Metall. Mater. Sci. Eng.*, vol. 5, no. 2, pp. 156–159, May 2000.
[19] L. L. Sun and P. Q. Wang, "Effect of temperature on back-EMF value of permanent magnet synchronous motor," *Automot. Electr. Appliance*, vol. 2, pp. 11–12, Feb. 2019.
[20] W. H. Zhang and J. H. Li, "Calculation formula of counter potential coefficient in design of brushless DC torque motor," *Small Special Elect. Mach.*, vol. 34, no. 1, pp. 43–44, Jan. 2006.
[21] F. G. Capponi, R. Terrigi, and G. De Donato, "A synchronous axial flux PM machine d,q axes model which takes into account iron losses, saturation and temperature effects on the windings and the permanent magnets," in *Proc. Int. Symp. Power Electron. (ISPE)*, May 2016, pp. 39–44.
[22] Z. X. Sun, "Research in performance and temperature rise of permanent magnet synchronous motor in high temperature environment," Ph.D. dissertation, Dept. Elect. Mach. App., Harbin Inst. Technol., Harbin, China, 2017.
[23] D. S. Gu, "Development of test system and study on transmission performance for harmonic gear drive," Ph.D. dissertation, Dept. Mech. Des. Theory, Harbin Inst. Technol., Harbin, China, 2014.
[24] W. T. Li, G. P. Sun, and N. Wang, "Parameter analysis of analytical dynamic model for hatch cover drive mechanism," *Manned Spaceflight*, vol. 24, no. 3, pp. 370–376, Jun. 2018.
[25] J. Sun, Q. P. Wen, and H. Zhou, "Lubrication and performance of harmonic drive used in spacecraft," *J. Astronaut.*, vol. 30, no. 1, pp. 378–381, Jan. 2009.
[26] K. Zhao, "Development of performance testing system of harmonic drive reducer under thermal vacuum environment," Ph.D. dissertation, Dept. Mech. Eng., Harbin Eng. Univ., Harbin, China, 2017.
[27] X. H. Li, J. K. Liu, and S. Wang, "Transmission performance test of harmonic gear lubricated with 601EF grease under vacuum thermal cycling environment," *Spacecraft Environ. Eng.*, vol. 28, no. 5, pp. 450–453, Oct. 2011.
[28] K. Maniwa and S. Obara, "Lubrication mechanism between wave generator and flexspline in strain wave gearing under in-vacuum and in-air environments: Measurement of contact electric resistance between mechanical elements," *J. Jpn. Soc. Tribol.*, vol. 52, no. 1, pp. 1–17, 2007.

PAN BO (M'05) was born in Harbin, Heilongjiang, China, in 1982. He received the B.S. and M.S. degrees in mechanical engineering from Beihang University, Beijing, China, in 2005 and 2007, respectively, and the Ph.D. degree from the China Academy of Space Technology, Beijing, China, in 2010. He is currently a Senior Engineer with the Beijing Institute of Spacecraft System Engineering.

CHI CHENG was born in Harbin, Heilongjiang, China, in 1995. He received the B.S. degree in mechanical engineering from the Harbin Institute and Technology, in 2017, where he is currently pursuing the master's degree in mechanical engineering with the School of Mechatronics Engineering.

HE YONGQIANG was born in Guyuan, Ningxia, China, in 1986. He received the B.S. and M.S. degrees in mechatronic engineering from the Beijing University of Posts and Telecommunications, Beijing, China, in 2008 and 2011, respectively. He is currently a Senior Engineer with the Beijing Institute of Spacecraft System Engineering.

ZHANG SHUYANG, photograph and biography not available at the time of publication.

ZHANG PUZHEN, photograph and biography not available at the time of publication.

ZHANG DONGHUA, photograph and biography not available at the time of publication.

CHI GUANXIN (M'89) was born in Hulin, Heilongjiang, China, in 1968. He received the B.S. and M.S. degrees in mechanical engineering from Harbin Science and Technology University, Harbin, China, in 1989 and 1992, respectively, and the Ph.D. degree in mechanical engineering from the Harbin Institute of Technology, Harbin, in 1999. From 1999 to 2002, he was a Postdoctoral Fellow of mechanical manufacturing and automation with the School of Mechatronics Engineering, HIT, where he has been a Professor with the Mechanical Engineering Department, School of Mechatronics Engineering, since 2011. He is the author of three books, more than 70 articles, more than ten inventions, and more than five software copyrights. He has completed or undertaken more than 20 scientific research projects, such as the national 863 plan, the natural science foundation, the national defense foundation pre-research, and the third phase of the lunar exploration project. He has developed multiple versions of multiaxis CNC system software based on Windows/Linux system. He was awarded the title of Outstanding Teacher of the School, in 2010 and Advanced Worker, in 2015. His research interests include high efficiency and energy saving EDM pulse power supply technology, EDM and micro-EDM technology, multiaxis CNC systems, and automatic control application.